Penerbit Akademia Baru

Journal of Advanced Research in Micro and Nano Engineering

Journal homepage: https://akademiabaru.com/submit/index.php/armne
ISSN: 2756-8210

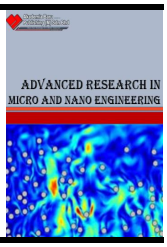

Passively Q-Switched Thulium-Holmium Doped Fibre Laser with Electrochemical Exfoliation Graphene in Chitin Based Passive Saturable Absorber

Nur Nadhirah Mohamad Rashid[1], Harith Ahmad[2], Mohammad Faizal Ismail[2], Siti Nur Fatin Zuikafly[1], Nur Azmah Nordin[1], Tsuyoshi Koga[3], Wira Jazair Yahya[1], Hafizal Yahaya[1], Fauzan Ahmad[1,*]

[1] Malaysia-Japan International Institute of Technology (MJIIT), Universiti Teknologi Malaysia, Jalan Sultan Yahya Petra, 54100 Kuala Lumpur, Malaysia
[2] Photonics Research Centre, University of Malaya, 50603 Kuala Lumpur, Malaysia
[3] Graduate School of Science and Engineering for Innovation, Yamaguchi University, 2-16-1 Tokiwadai, Ube City, Yamaguchi 755-8611, Japan

ABSTRACT

Recent years saw low-dimensional carbon nanostructures like graphene as excellent saturable absorber (SA) for its unique electric and optical properties. Graphene exhibits ultrafast recovery times and high damage thresholds and can be manufactured by relatively simple methods. In this work, graphene was synthesized using the electrochemical exfoliation (ECE) method. Chitin biopolymer was used to develop graphene-based SA as a more environmentally friendly alternative to conventional synthetic polymers. The fabricated passive SA was then integrated into Thulium-Holmium-doped fibre laser (THDFL) in ring cavity for pulsed laser generation via Q-switching. The optical and physical properties of the graphene-based SA were characterized using Raman spectroscopy, field emission scanning electron microscopy (FESEM) and energy-dispersive x-ray spectroscopy (EDS). Q-switched pulse was successfully demonstrated using the fabricated graphene SAs. ECE graphene-chitin SA generated a Q-switched pulse region at 2 µm with the repetition rate and shortest pulse width of 67.78 kHZ and 10.03 µs, respectively. The signal-to-noise ratio (SNR) values obtained was 40 dB indicating high stability of the pulse laser-generated. This study demonstrated the potential of graphene embedded in chitin biopolymer as a sustainable and environmentally friendly SA for a wide range of applications, particularly for pulsed fibre lasers.

Keywords:
Saturable absorber; Thulium-Holmium doped fibre; Graphene; Chitin

Received: 17 Dec. 2022	Revised: 12 Jan. 2023	Accepted: 15 Jan. 2023	Published: 28 Jan. 2023

1. Introduction

Recently, discovering new materials to act as SAs for passive Q-switching applications in fibre lasers has piqued interest. Significant research has been conducted in this regard to develop a less expensive and less complex alternative to the use of SESAMs for passive Q-switching [1]. Recent years saw low-dimensional carbon nanostructures like carbon nanotubes (CNTs) and graphene as excellent SAs for their unique electric and optical properties [2]. Graphene has ultrafast and slow recovery from

* *Corresponding author*
Email address: fauzan.kl@utm.my

https://doi.org/10.37934/armne.11.1.114

saturation and they exhibit fast and slow saturation recovery [3]. The stability, cost, and properties of graphene are strongly influenced by the fabrication processes. Various fabrication techniques have been developed since the first successful fabrication of 2D graphene from its bulk form using a mechanical exfoliation (ME) method using scotch tape [4]. ME is a straightforward yet approachable method for producing high-quality monolayers or few-layer graphene by repeatedly exfoliating bulk crystals with adhesive tape. However, there are obvious drawbacks: it's extremely low output/yield and uncontrollability are not suitable for large-scale production or applications [5,6]. Chemical vapour deposition (CVD), as compared to ME, produces less damage [7]. The CVD method produces a more uniform material on a better-quality substrate than the ME. However, flake transfer requires a hot substrate temperature and is more complex and costly [8]. Toxic liquids and polymers make this method's etching challenging.

Due to the disadvantages of these fabrication techniques, this paper proposes an approach for producing graphene-based SA via an electrochemical exfoliation technique. Graphene-based SA fabrication can be accomplished at room temperature with simple and efficient procedures using minimal apparatus and materials. Graphene generated via the electrochemical exfoliation process was homogenized with a host polymer to facilitate integration into the laser cavity. Although polyvinyl alcohol (PVA), polymethyl methacrylate (PMMA), and sodium carboxymethyl cellulose (Na-CMC) biopolymer composites were frequently used as the SA film host polymers, these materials have several drawbacks, such as Na-CMC's susceptibility to moisture and the low glass transition temperatures of PMMA (105°C) and PVA (85°C), which limit the thermal stability [9].

Given its biochemical properties, including biodegradability, non-toxicity, biocompatibility, and the capacity to form films, chitin biopolymer is an alternative to the synthetic host polymer [10,11]. Additionally, chitin is tough and durable in high-acidity and harmful environments, making it useful for producing films that can be used in high-power and high-temperature laser operations. This has been a problem for existing SAs since the performance of the SA is often constrained by the host polymer's low heat resistance. This advantage has prompted the use of chitin in the fabrication of CNT-chitin-based SAs for pulsed laser generation [12]. Even though graphene-based SAs have been extensively studied, their passive mode-locking and soliton-generating capacity in a wavelength 2 μm region of the short-wave infrared has yet to be fully explored.

Therefore, an electrochemical exfoliation (ECE) graphene embedded with chitin biopolymer composite SA was fabricated and incorporated in thulium-holmium doped fibre lasers (THDFL) and its pulse fibre laser performance is investigated.

2. Methodology

2.1 Fabrication of SA Films

The graphene flakes produced through the electrochemical exfoliation process of graphite rods. Two electrodes of graphite will be placed 1 cm apart in a beaker containing an electrolysis cell with 1 % of sodium dodecyl sulphate (SDS) in de-ionized (DI) water). Surfactant is used for its capacity to prevent the agglomeration of the exfoliated graphene. The stress induced by the intercalation of large sulphate ions into the anode weakens the graphene layers' bond, assisting in the exfoliation of the graphene. The electrodes was supplied with a decomposition potential of 20 V. The electrolysis of water at the electrodes is expected to induce the production of oxygen and hydroxyl radicals which will eventually cause the graphene to loosen the graphite rods. The chemical reactions involved are shown in Eq. (1) and Eq. (2) [13]

$$H_2O \rightarrow OH^- + H^+ \quad (1)$$

$$CH_3(CH_2)_{11}OSO_3Na \rightarrow CH_3(CH_2)_{11}OSO_3^+ + Na^+ \quad (2)$$

The hydrogen and oxygen gas were encapsulated within microbubbles with the presence of SDS in electrolyte and assisted in exfoliating the graphite, producing the graphene flakes. The exfoliation process was continued for 2 hours to attain a stable graphene solution in the SDS solution. The stable graphene solution was then centrifuged at 1000 rpm for 30 minutes (SIGMA 4-5L benchtop centrifuge). Then the supernatant of the graphene suspension was decanted due to the size of graphene flakes, making it easier to bind homogeneously within the host polymer matrices for fabrication of the saturable absorber.

The preparation of the chitin polymer was performed following the procedure of Nawawi *et al*., [14]. Pleurotus ostreatus mushrooms were thawed and rinsed with distilled water for 5 min to remove any observable contaminants. After rinsing three times, the mushrooms were blended for 5 mins using a commercial kitchen blender. An extraction process was performed using hot water at 85°C for 30 mins to remove any water-soluble components. Excess water containing soluble components was then removed by centrifugation, and the residual mushroom cake was soaked in 1 M NaOH to remove protein, lipid and alkaline-soluble polysaccharides, re-centrifuged to remove excess solids, and diluted in water (0.8% w/v) before being stored at 4°C for further use.

To prepare the ECE graphene-chitin SA, the graphene flakes suspension was mixed with the chitin in one-to-four ratio (25%: 75%) to sum up to 5 ml. The 5 mL amount was chosen as the amount is suitable for the circular petri dish with a 3.5 cm diameter and 1.0 cm height. This resulted in a strong and sturdy film with a thickness of around 30 µm to 50 µm which makes it easier for the SA to be peeled off later. The mixture of ECE graphene, with chitin, was ultrasonicated for 60 mins to ensure that the ECE graphene was evenly dispersed in the chitin. The mixture was then transferred to a petri dish and left to dry for 48 h at room temperature, resulting in a free-standing graphene-chitin-based SA film as shown in Figure 1.

Fig. 1. ECE graphene-chitin film

2.2 Experimental Setup for Fibre Laser Generation

The experimental setup for the Q-switched thulium-holmium-doped fibre laser (THDFL) is depicted in Figure 2. Two laser diodes (CLD1015, Thorlab) with 1550 nm centre wavelengths were used to pump the gain medium, which was a 1.5 m thulium-holmium doped fibre (THDF). To maintain unidirectional laser operation, 1550 nm polarization-insensitive isolators (PI-ISO) were placed at both

ends of the amplifier section. A 1550/2000 nm WDM was placed after each 1550 nm PI-ISO to guide the 1550 nm pumped light to the gain medium. A 2000 nm PI-ISO was placed after the WDM to allow the light to propagate only in the clockwise direction. The free-standing SA (1 mm × 1 mm) was then sandwiched between two fibre ferrules inside a fibre connecter/physical contact (FC/PC) to act as passive Q-switcher. The propagated light was then extracted from the cavity using a 90/10 optical coupler. The THDFL cavity consisted of a 13 m single-mode fibre laser (SMF) and 1.5 m of THDF. The output signal was measured using a 500 MHz digital oscilloscope (DLM 2054, Yokogawa) with a 12.5 GHz InGaAs photodetector (818-BB-51F, Newport), an optical spectrum analyzer (OSA) (AQ6370, Yokogawa) with a resolution of 0.2 nm, an optical power meter (OPM) (PM100USB, Thorlabs), an autocorrelator (PulseCheck 150, APE), and a radio frequency spectrum analyzer (RFSA) (FSC 6, Rohde & Schwarz). This equipment was used to measure the pulse train, operating wavelength, output power, pulse width and signal to noise ratio (SNR) of the generated pulse, respectively.

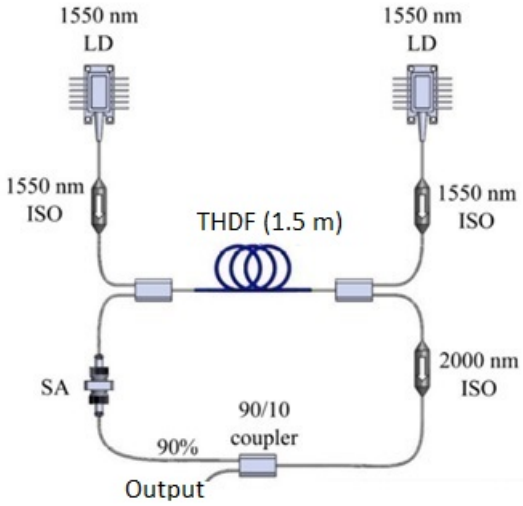

Fig. 2. Experimental setup of THDFL

2.3 Structural Characterization

Field emission scanning electron microscopy (FESEM) analysis was performed to observe the surface morphology of the fabricated samples. FESEM analysis was performed using FESEM (JSM-7800F, JEOL). Before performing FESEM analysis, the fabricated samples were coated with platinum using auto fine coater (JEC-300FC, JEOL). Coating of samples is required to reduce thermal damage, enhance secondary electron emission and prevent charging of the specimen, which would otherwise occur due to the accumulation of the static electric field. It happens mainly for non-conducting or beam-sensitive samples.

Figure 3 shows the FESEM images of ECE graphene with and without host polymer chitin. Figure 3(a) shows the FESEM image of ECE graphene in bundled form. Meanwhile, Figure 3(b) shows a thoroughly mixed ECE graphene in chitin polymer with a smooth surface and low aggregation. There are no obvious air holes or bubbles in the polymer films, which indicates the excellent uniformity of the fabricated SA.

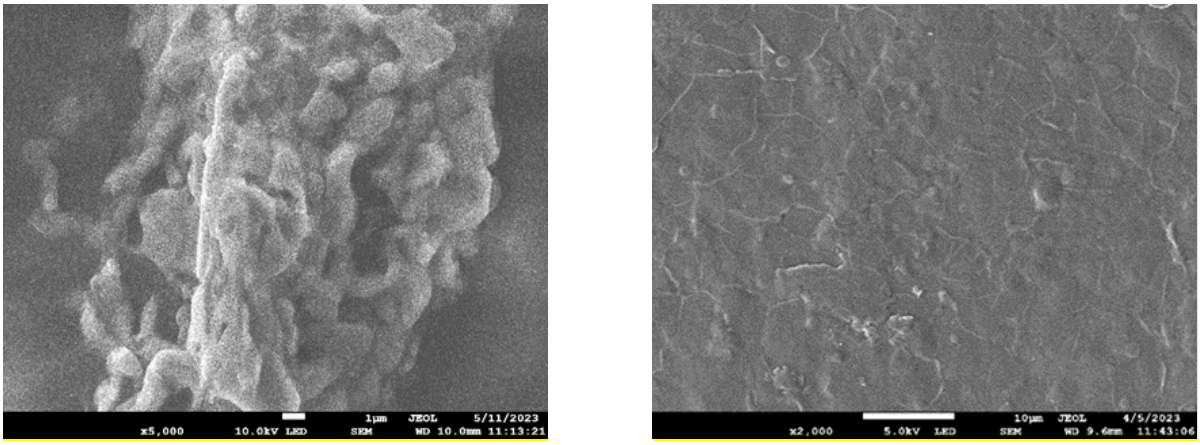

(a) (b)

Fig. 3. FESEM image of (a) ECE graphene, (b) ECE graphene-chitin

The composition of the ECE graphene with and without the host polymer was evaluated using EDS as shown in Figure 4 (a)-(b). The element composition for each sample is shown in the inset of Figure 4 (a)-(b). The presence of carbon (C) and oxygen (O) elements confirmed the existence of ECE graphene, meanwhile, sodium (Na) and sulphur (S) elements are from the SDS solution during the fabrication process which shows by their lower weights' percentage. The presence of all these elements confirmed that the fabrication of ECE graphene is successful. The existence of the platinum (Pt) element is due to the sample being coated before the FESEM analysis.

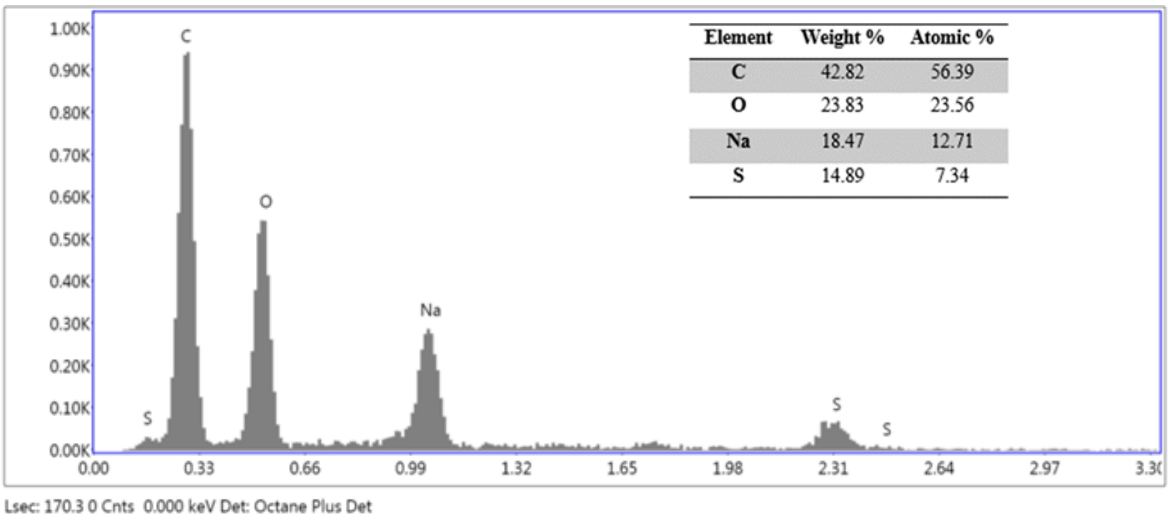

Element	Weight %	Atomic %
C	42.82	56.39
O	23.83	23.56
Na	18.47	12.71
S	14.89	7.34

(a)

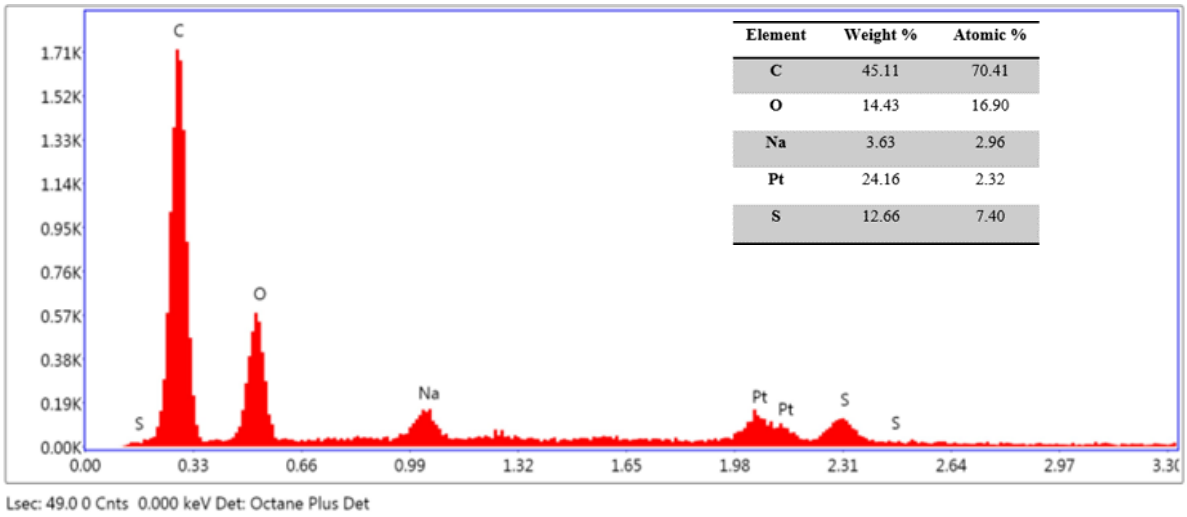

Element	Weight %	Atomic %
C	45.11	70.41
O	14.43	16.90
Na	3.63	2.96
Pt	24.16	2.32
S	12.66	7.40

(b)

Fig. 4. EDS spectrum of (a) ECE graphene, (b) ECE graphene-chitin

The thickness of the fabricated SA is then measured by a 3D measuring laser microscope (LEXT OLS4100, OLYMPUS). Figure 5 shows the 3D laser images taken from ECE graphene embedded with chitin host polymer. The measurement was taken at three distinct points on the films and the average thickness was shown in Figure 5. The film thickness was reported at ~ 72.05 µm, nevertheless, a thicker film means more absorption due to graphene loading thus it takes a longer time for the SA to bleach and thus the repetition rate fibre laser is usually lower [15].

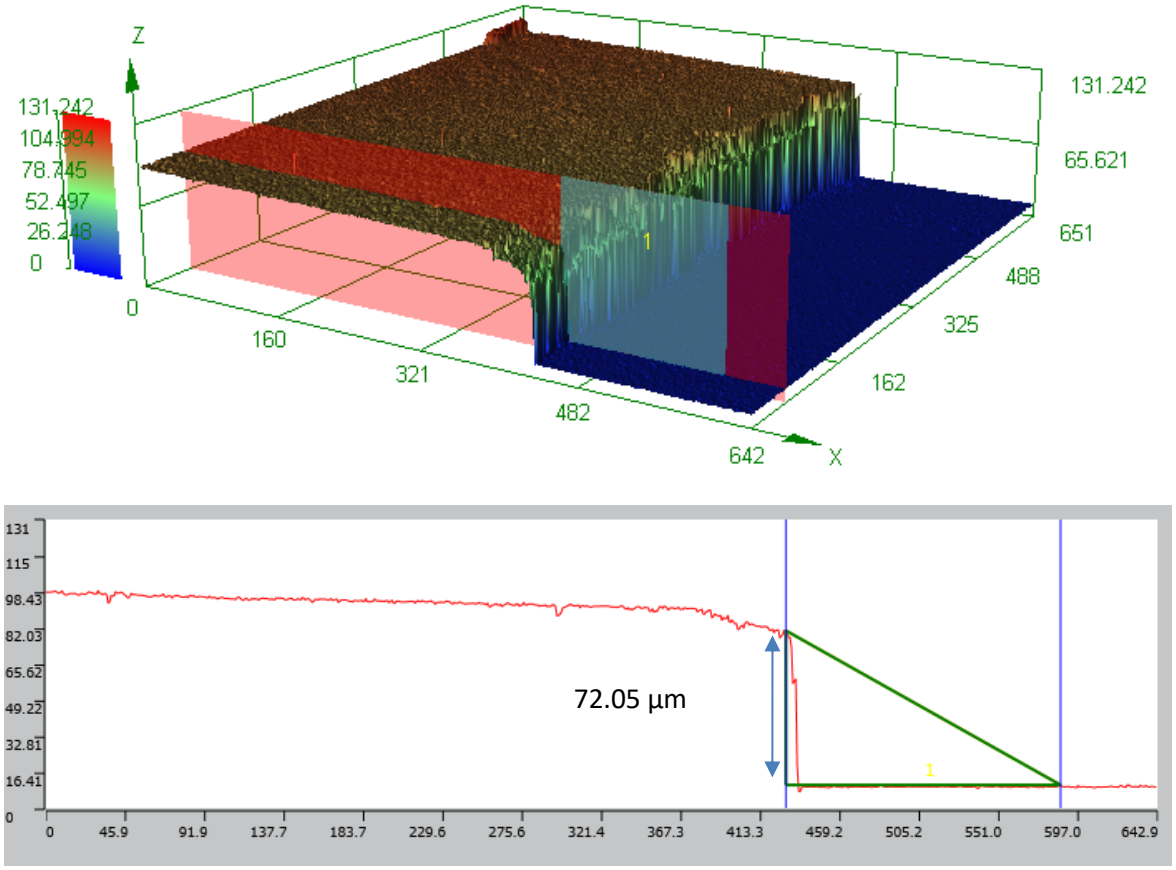

Fig. 5. ECE graphene-chitin film's thickness

2.4 Raman Measurement

Figure 6 shows the Raman spectrum representing the vibrational properties of the fabricated graphene SAs, obtained via Raman spectroscopy (Witec, Alpha 300R) through a 488 nm laser source at room temperature. Raman spectroscopy was performed with graphene samples to determine the quality of the epitaxial graphene as well as to confirm the number of graphene layers. The signature of D and G of graphene were observed in 1136 cm^{-1} and 1587 cm^{-1} for ECE graphene-chitin which confirm the low defect content in the graphitic structure.

Raman signature of single-layer graphene includes most of the features that exist within all carbon-based materials such as graphite, CNT, GO and rGO. For example, the Raman signature of single-layer graphene contained two distinct features that one cannot see in even two-layer. The first one is the small upshift of about 5 cm^{-1} of the "G" peaks and the second is the improvement that happens in the graphite shoulder peak to second order "D" peak [16]. The "2D" band at 3089 cm^{-1} and 2882 cm^{-1}, which originates from a two-phonon double resonance Raman process and is indicative of crystalline graphitic materials, are highly sensitive to the number of graphene layers and has been utilised to distinguish the single-layer from few-layer graphene [17].

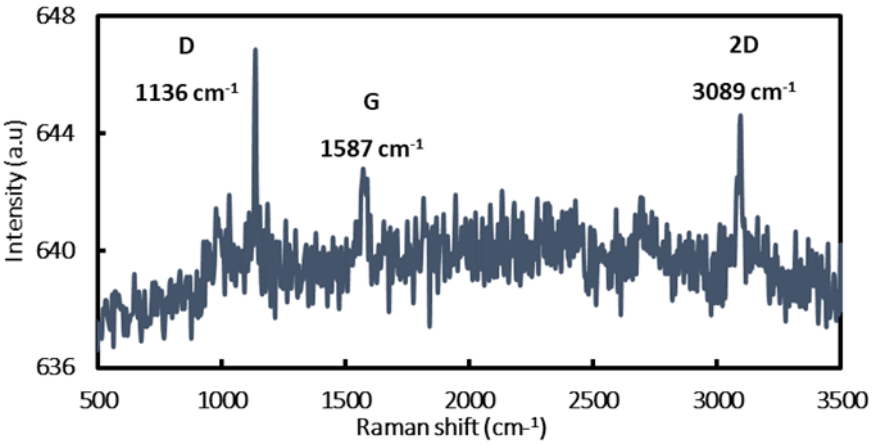

Fig. 6. Raman spectrum of ECE graphene-chitin SA

2.5 Nonlinear Optical Measurement

The nonlinear optical properties of the ECE graphene-chitin SA were then measured using power-dependent absorption measurement. The nonlinear properties of SAs were measured using a twin detection method. A commercial Toptica FemtoFerb 1950 fs laser was utilized as the laser source for the 2.0 µm region with a centre wavelength of 1950 nm, a fundamental frequency of 30 MHz, and a pulse duration of 100 fs. During the measurement, the light source was connected to the optical attenuator to attenuate the incoming signal. The output was then split using a 3-dB optical coupler in which one of the ports was connected to the SA and another to an optical power meter (OPM) as a reference. The output power of both of the detectors was recorded using OPMs as the attenuation value gradually decreased. Figure 7 shows the measurement setup for the modulation depth at the 2 µm wavelength. The power-dependent absorption measurement was then calculated and fitted using Eq. (3.2) [18]

$$\alpha(I) = \frac{\alpha_o}{1+\frac{I}{I_{sat}}} + \alpha_{ns} \quad (3)$$

where $\alpha(I)$ is the intensity-dependent absorption coefficient, and α_o, α_{ns}, and I_{sat} are the saturable absorption (modulation depth), non-saturable absorption and saturation intensity, respectively.

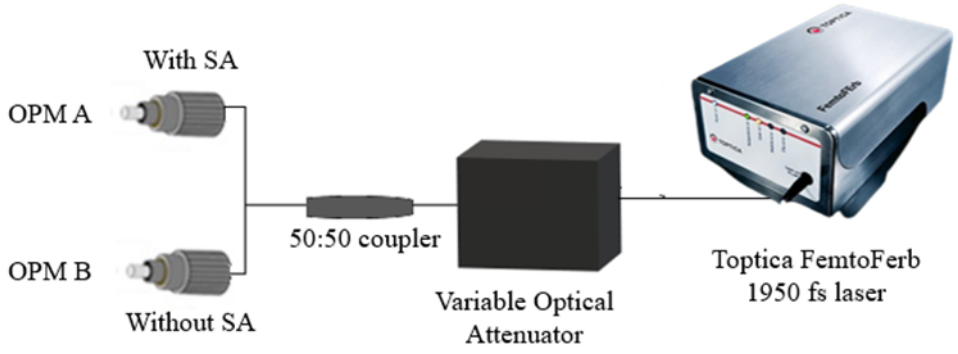

Fig. 7. Nonlinear optical measurement setup

Modulation depth for ECE graphene-chitin was calculated as 9.7% as shown in Figure 8, respectively. The modulation depth obtained by graphene in this work is smaller than the modulation depth obtained by Wang *et al.,* where the modulation depth is 40.27% [19]. The large modulation depth SAs were prepared through the CVD method. The high value of non-saturable losses is attributed to the residual absorption of amorphous carbon, metal catalysts, and graphene is not resonant with the incident light. In addition, scattering from the residual bundles and unevenness of the surface of the sample may also lead to an increase in non-saturable loss, which could weaken the performance of a mode−locked laser due to a higher threshold and lower output [18,20].

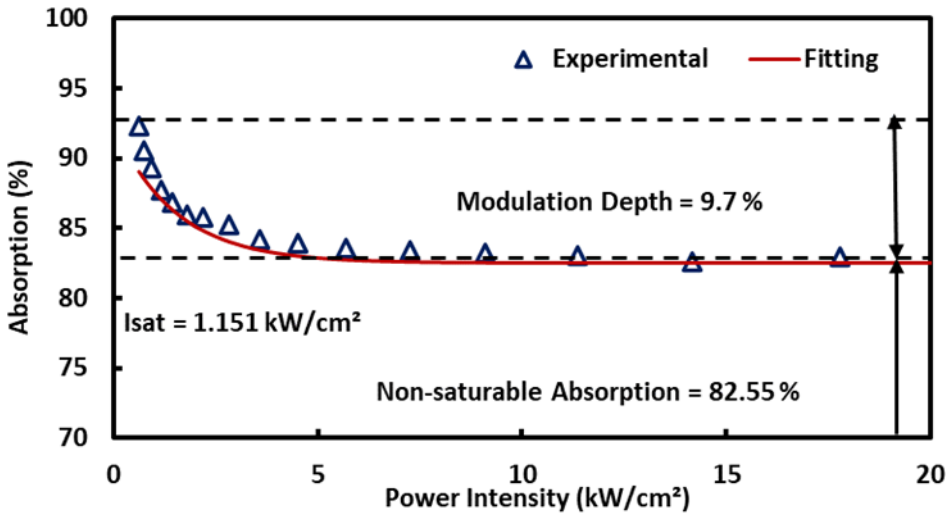

Fig. 8. Non-linear measurement of ECE graphene-chitin SA

3. Experimental Results

Figure 9 shows the optical spectrum trace without and with saturable absorber of ECE graphene-chitin SA at maximum input pump power of 398 mW. Incorporating the SA into the laser cavity enables the laser to operate at approximately 2 µm. The 3-dB bandwidth with a SA was around 6.6 nm, as shown in Figure 9. Stable Q-switched performance was gained once the pump power was above a threshold level of 307.6 mW and remained stable as the pump power was increased up to

the maximum power of the pump laser, which was 398 mW. The operating wavelength of the Q-switched laser has shifted to a shorter wavelength than the CW laser (without SA). This is due to increased cavity loss with the addition of SA. To compensate for the loss, the pulsating light in the cavity shifts to a shorter wavelength closer to the peak absorption of the THDF at roughly 1900 nm. The self-phase modulation effect in the ring cavity additionally broadens the spectrum bandwidth in the Q-switched laser.

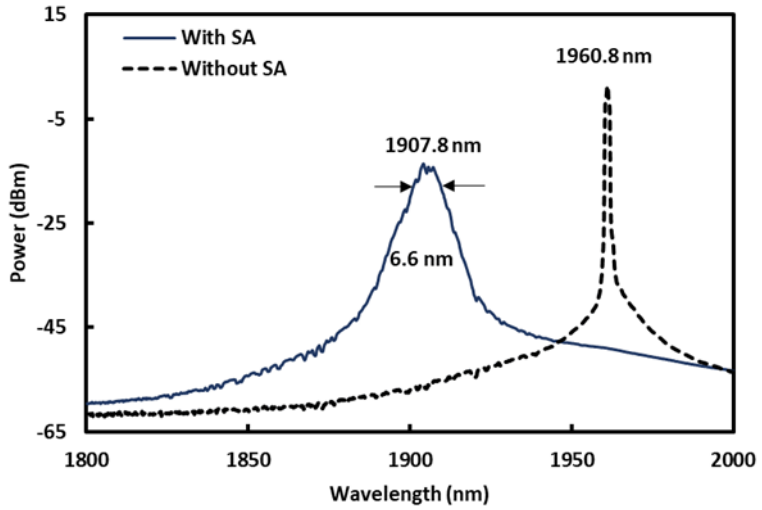

Fig. 9. Optical spectrum trace at maximum input pump power without and with SA

Figure 10 shows that the pulses had a repetition rate of 67.78 kHz with a pulse-to-pulse separation of 15 µs. Meanwhile, the pulse width was 10.03 µs, as observed in Figure 10. Each Q-switched pulse envelope had an asymmetric intensity profile with no amplitude modulation demonstrating that the self-mode locking phenomenon had been effectively controlled. Shortening the length of the laser resonator, such as using a shorter gain fibre length with a high doping level, may lead to a shorter pulse duration [21].

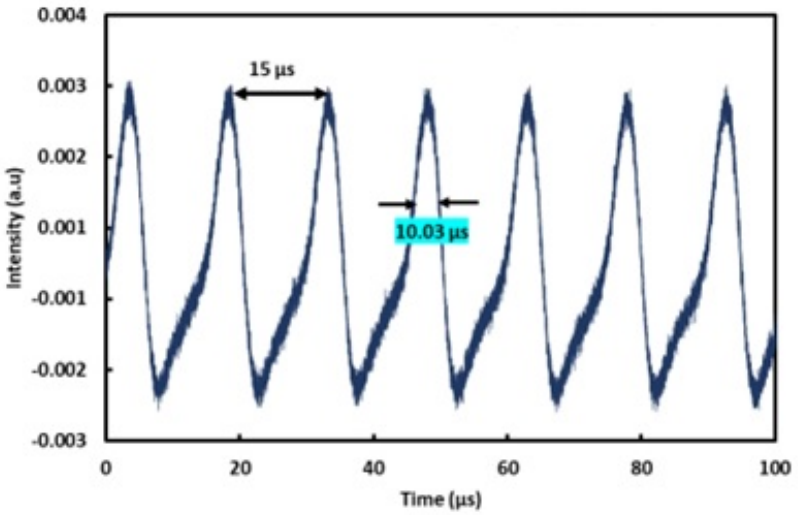

Fig. 10. A Q-switched pulse train at a pump power of 398 mW with pulse-to-pulse separation of 15 µs and pulse width of 10.03 µs

Figure 11 depicts the relationship between repetition rate, pulse width, and pump power. Q-switched pulse repetition rate varied with pump power, unlike mode-locked fibre lasers, whose repetition rate depended on cavity length [22,23]. Increasing the pump's power increases the repetition rate from 52.3 kHz to 67.78 kHz. The repetition rate obtained is higher than the repetition rate obtained by previous work of ECE graphene-PEO and GO-PVA SA [24,25]. The pulse width decreased from 13.29 µs to 10.03 µs as the pump power increased from 307.6 mW to 398 mW. As more pump power was pumped into the cavity, the gain population was excited to a saturation state more rapidly. This enabled a shorter pulse width at a faster pulse repetition rate. The pulse width and repetition rate patterns were consistent with the passive Q-switching theory [26].

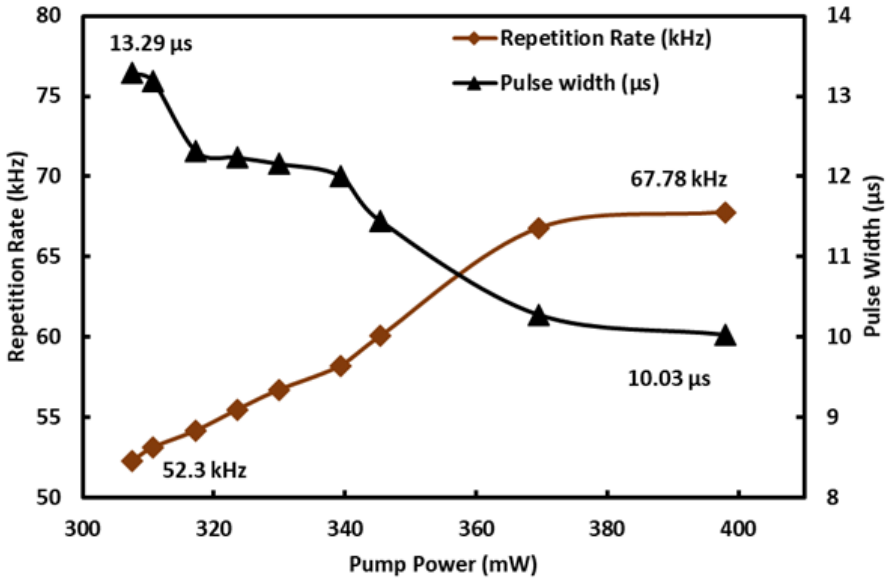

Fig. 11. Pulse width and repetition rate as a function of pump power

Figure 12 shows the pulse energy and peak power of ECE graphene embedded with chitin polymer as a function of pump power. Increasing the pump power from 307.6 mW to 398 mW increased the pulse energy from 54.68 nJ to 83.95 nJ. The peak power also showed a similar pattern to that of pulse energy, where the peak power was increased from 3.87 mW to 7.87 mW. The pulse energy of this work is higher than the pulse energy obtained in previous work [21].

The ECE graphene-chitin SA's radio frequency spectrum analyzer (RFSA) trace is shown in Figure 13. As can be observed, the signal to noise ratio (SNR) ratio at a pump power of 398 mW was 39.48 dB. This SNR value showed that the Q-switched pulse laser operated at good stability, indicating the ECE graphene-chitin-based SA able to generate a stable pulsed.

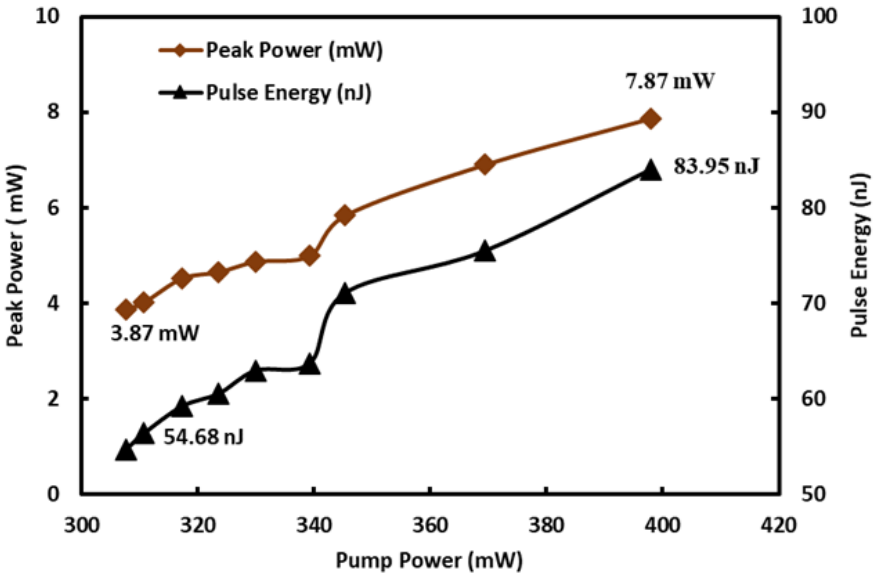

Fig. 12. Pulse peak power and pulse energy as a function of pump power

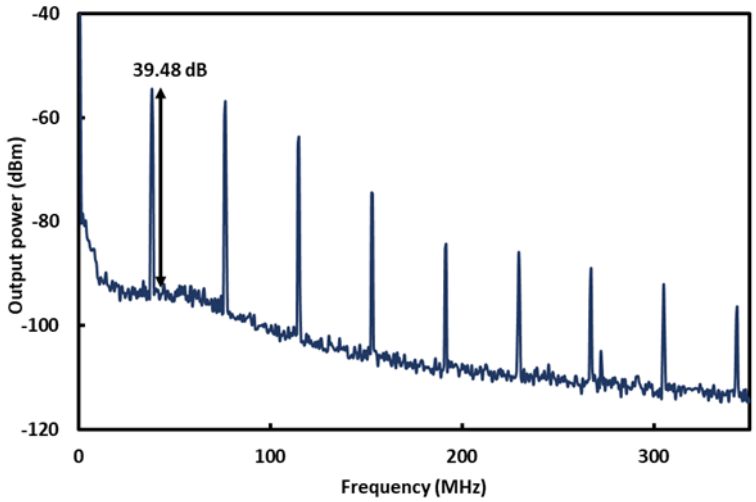

Fig. 13. RFSA measurement signal-to-noise ratio at a pump power of 398 mW

Table 1 summarises the comparison of Q-switcher performances of the fabricated SAs in the 2 μm region. The threshold pump power of ECE graphene-chitin is lower than most of the values reported in Table 1. Aside from the high nonlinear response of graphene, which enhances the absorption of photons, the use of chitin in this case compared to other synthetic polymers reduces the pump power needed to achieve Q-switched operation due to its reduced saturation fluence, as chitin has low saturation intensity. Since it is known that the choice of host polymer can affect the packing density and orientation of the SA molecules, which in turn can affect the nonlinear optical response and saturation fluence, chitin can be said to be more compatible with the base material [27].

Table 1
Comparison of all-fibre Q-switched lasers operating in 2.0 µm region

Material	λ_C (nm)	Pump power (mW)	Pulse width (µs)	Repetition rate (kHz)	Peak power (mW)	Pulse energy (nJ)	SNR (dB)	Output power	Ref
GO-PVA	1944	344–491	5.08–4.2	15.76–25.08	151.6	0.68	49	17	[25]
SWCNT-PVA	1967	3600	~0.87	85–164	-	630	-	103	[21]
Titanium-PVA	1552	272.1–467	5.62–2.22	21.8–39.1	55.8	124	55	1.63–4.84	[28]
MOS_2-PVA	2032	2890–3410	2.06–1.76	33.6–48.1	-	1000	54.6	47.3	[29]
ECE graphene-chitin	1907.8	307.6–398	13.29–10.03	52.3–67.78	3.87–7.86	54.68–83.95	39	2.86–5.69	This study

Graphene filament embedded with chitin polymer has a higher repetition rate compared to other based materials in Table 1. The pulse width of graphene filament-chitin is higher than those values in Table 1 and comparable to GO-PVA SA in Table 1. Furthermore, the SNR value of this work, which is higher compared to those reported in Table 1, suggests that graphene embedded in chitin can improve the performance of SAs in laser applications. Overall, laser performance in this study was better than most if not all related previous studies, as shown in Table 41. This shows the potential of graphene chitin-based SAs for multiple applications in the 2 µm region, such as medical surgery, free-space optical communications, light detection and ranging (LIDAR), nonlinear frequency conversion, and transparent material processing.

4. Conclusions

This study investigated the fabrication of graphene through the cost-efficient electrochemical exfoliation method with chitin as a host polymer. The synthesised ECE graphene embedded with chitin was employed in a pulsed laser cavity in the wavelength region of 2 µm to enable Q-switching pulse laser operations. The experimental result produced pulse peak power and pulse energy of 7.86 mW and 83.95 nJ. The pump power produced a maximum repetition rate of 67.78 kHz with the shortest pulse width of 10.03 µs when increased from 307.6 mW to 398 mW.

References

[1] Keller, Ursula. "Recent developments in compact ultrafast lasers." *nature* 424, no. 6950 (2003): 831-838. https://doi.org/10.1038/nature01938
[2] Woodward, Robert I., and Edmund JR Kelleher. "2D saturable absorbers for fibre lasers." *Applied Sciences* 5, no. 4 (2015): 1440-1456. https://doi.org/10.3390/app5041440
[3] Sobon, Grzegorz. "Application of 2D materials to ultrashort laser pulse generation." *Two-dimensional Materials-Synthesis, Characterization and Potential Applications 1* (2016). https://doi.org/10.5772/63336
[4] Novoselov, Kostya S., Andre K. Geim, Sergei V. Morozov, De-eng Jiang, Yanshui Zhang, Sergey V. Dubonos, Irina V. Grigorieva, and Alexandr A. Firsov. "Electric field effect in atomically thin carbon films." *science* 306, no. 5696 (2004): 666-669. https://doi.org/10.1126/science.1102896
[5] Bhuyan, Md Sajibul Alam, Md Nizam Uddin, Md Maksudul Islam, Ferdaushi Alam Bipasha, and Sayed Shafayat Hossain. "Synthesis of graphene." *International Nano Letters* 6 (2016): 65-83. https://doi.org/10.1007/s40089-015-0176-1
[6] Peng, Xi, and Yixin Yan. "Graphene saturable absorbers applications in fiber lasers." *Journal of the European Optical Society-Rapid Publications* 17, no. 1 (2021): 16. https://doi.org/10.1186/s41476-021-00163-w

[7] Yin, Jinde, Jiarong Li, Hao Chen, Jintao Wang, Peiguang Yan, Mengli Liu, Wenjun Liu et al. "Large-area highly crystalline WSe 2 atomic layers for ultrafast pulsed lasers." *Optics express* 25, no. 24 (2017): 30020-30031. https://doi.org/10.1364/OE.25.030020

[8] Chen, Hao, Jinde Yin, Jingwei Yang, Xuejun Zhang, Mengli Liu, Zike Jiang, Jinzhang Wang et al. "Transition-metal dichalcogenides heterostructure saturable absorbers for ultrafast photonics." *Optics letters* 42, no. 21 (2017): 4279-4282. https://doi.org/10.1364/OL.42.004279

[9] Kang, Daewon, Sourav Sarkar, Kyung-Soo Kim, and Soohyun Kim. "Highly Damage-Resistant Thin Film Saturable Absorber Based on Mechanically Functionalized SWCNTs." *Nanoscale Research Letters* 17, no. 1 (2022): 11. https://doi.org/10.1186/s11671-021-03648-2

[10] Elieh-Ali-Komi, Daniel, and Michael R. Hamblin. "Chitin and chitosan: production and application of versatile biomedical nanomaterials." *International journal of advanced research* 4, no. 3 (2016): 411.

[11] Shervani, Zameer. "Chitin-gold nanocomposite film and electro-optical properties." *Front. Nanosci. Nanotechnol* 3, no. 3 (2017): 2-4. https://doi.org/10.15761/FNN.1000158

[12] Zuikafly, Siti Nur Fatin, Harith Ahmad, Mohd Faizal Ismail, Mohd Azizi Abdul Rahman, Wira Jazair Yahya, Nurulakmar Abu Husain, Khairil Anwar Abu Kassim, Hafizal Yahaya, and Fauzan Ahmad. "Dual Regime Mode-Locked and Q-Switched Erbium-Doped Fiber Laser by Employing Graphene Filament–Chitin Film-Based Passive Saturable Absorber." *Micromachines* 14, no. 5 (2023): 1048. https://doi.org/10.3390/mi14051048

[13] Lu, Jiong, Jia-xiang Yang, Junzhong Wang, Ailian Lim, Shuai Wang, and Kian Ping Loh. "One-pot synthesis of fluorescent carbon nanoribbons, nanoparticles, and graphene by the exfoliation of graphite in ionic liquids." *ACS nano* 3, no. 8 (2009): 2367-2375. https://doi.org/10.1021/nn900546b

[14] Fazli Wan Nawawi, Wan Mohd, Koon-Yang Lee, Eero Kontturi, Richard J. Murphy, and Alexander Bismarck. "Chitin nanopaper from mushroom extract: natural composite of nanofibers and glucan from a single biobased source." *ACS Sustainable Chemistry & Engineering* 7, no. 7 (2019): 6492-6496. https://doi.org/10.1021/acssuschemeng.9b00721

[15] Harun, Sulaiman Wadi, M. A. Ismail, F. Ahmad, M. F. Ismail, Roslan Md Nor, N. R. Zulkepely, and Harith Ahmad. "A Q-switched erbium-doped fiber laser with a carbon nanotube based saturable absorber." *Chinese Physics Letters* 29, no. 11 (2012): 114202. https://doi.org/10.1088/0256-307X/29/11/114202

[16] Shakaty, Aseel A., Jassim K. Hmood, and Bushra R. Mhdi. "Graphene-based saturable absorber for pulsed fiber laser generation." In *Journal of Physics: Conference Series*, vol. 1795, no. 1, p. 012048. IOP Publishing, 2021. https://doi.org/10.1088/1742-6596/1795/1/012048

[17] Calizo, Irene, Alexander A. Balandin, Wenzhong Bao, Feng Miao, and C. N. Lau. "Temperature dependence of the Raman spectra of graphene and graphene multilayers." *Nano letters* 7, no. 9 (2007): 2645-2649. https://doi.org/10.1021/nl071033g

[18] Wang, Frank, A. G. Rozhin, V. Scardaci, Z. Sun, F. Hennrich, I. H. White, William I. Milne, and Andrea C. Ferrari. "Wideband-tuneable, nanotube mode-locked, fibre laser." *Nature nanotechnology* 3, no. 12 (2008): 738-742. https://doi.org/10.1038/nnano.2008.312

[19] Wang, Pengchao, Qi Yang, and Xiaoyang Wang. "Gold nanostars as the saturable absorber for a Q-switched visible solid-state laser." *Applied Optics* 58, no. 25 (2019): 6733-6736. https://doi.org/10.1364/AO.58.006733

[20] Dai, Lilong, Zinan Huang, Qianqian Huang, Chang Zhao, Aleksey Rozhin, Sergey Sergeyev, Mohammed Al Araimi, and Chengbo Mou. "Carbon nanotube mode-locked fiber lasers: recent progress and perspectives." *Nanophotonics* 10, no. 2 (2020): 749-775. https://doi.org/10.1515/nanoph-2020-0446

[21] Ma, H. F., Y. G. Wang, W. Zhou, J. Y. Long, D. Y. Shen, and Y. S. Wang. "A passively Q-switched thulium-doped fiber laser with single-walled carbon nanotubes." *Laser Physics* 23, no. 3 (2013): 035109. https://doi.org/10.1088/1054-660X/23/3/035109

[22] Zhang, L., J. T. Fan, J. H. Wang, J. M. Hu, M. Lotya, G. Z. Wang, R. H. Li et al. "Graphene incorporated Q-switching of a polarization-maintaining Yb-doped fiber laser." *Laser Physics Letters* 9, no. 12 (2012): 888. doi: 10.7452/lapl.201210090

[23] Wang, Tianxing, Zhijun Yan, Chengbo Mou, Zuyao Liu, Yunqi Liu, Kaiming Zhou, and Lin Zhang. "Narrow bandwidth passively mode locked picosecond Erbium doped fiber laser using a 45° tilted fiber grating device." *Optics Express* 25, no. 14 (2017): 16708-16714. https://doi.org/10.1364/OE.25.016708

[24] Saidin, N., D. I. M. Zen, B. A. Hamida, S. Khan, Harith Ahmad, K. Dimyati, and Sulaiman Wadi Harun. "A Q-switched thulium-doped fiber laser with a graphene thin film based saturable absorber." *Laser Physics* 23, no. 11 (2013): 115102. https://doi.org/10.1088/1054-660X/23/11/115102

[25] Kasim, Nabilah, Anas Abdul Latiff, Muhammad Farid Mohd Rusdi, M. B. Hisham, Sulaiman Wadi Harun, and Nor Farhah Razak. "Short-pulsed Q-switched Thulium doped fiber laser with graphene oxide as a saturable absorber." *Optik* 168 (2018): 462-466. https://doi.org/10.1016/j.ijleo.2018.04.117

[26] Ahmad, Harith, M. Suthaskumar, Zian Cheak Tiu, A. Zarei, and Sulaiman Wadi Harun. "Q-switched Erbium-doped fiber laser using MoSe2 as saturable absorber." *Optics & Laser Technology* 79 (2016): 20-23. https://doi.org/10.1016/j.optlastec.2015.11.007

[27] Zuikafly, S. N. F., Harith Ahmad, WMF Wan Nawawi, H. Yahaya, M. H. Ibrahim, A. A. Latif, and F. Ahmad. "Graphene-chitin bio-composite polymer based mode locker at 2 micron region." *Optik* 245 (2021): 167710. https://doi.org/10.1016/j.ijleo.2021.167710

[28] Muhammad, Ahmad Razif, Rozalina Zakaria, Muhammad Taufiq Ahmad, Hazli Rafis Abdul Rahim, Hamzah Arof, and Sulaiman Wadi Harun. "Q-Switched Thulium-Doped Fiber Laser with Pure Titanium-Film-Based Saturable Absorber." *Fiber and Integrated Optics* 38, no. 2 (2019): 137-147. https://doi.org/10.1080/01468030.2019.1575998

[29] Luo, Zhengqian, Yizhong Huang, Min Zhong, Yingyue Li, Jianyu Wu, Bin Xu, Huiying Xu, Zhiping Cai, Jian Peng, and Jian Weng. "1-, 1.5-, and 2-μm fiber lasers Q-switched by a broadband few-layer MoS^2 saturable absorber." *Journal of Lightwave Technology* 32, no. 24 (2014): 4077-4084. https://doi.org/10.1109/JLT.2014.2362147